Raman scattering and perturbed phonons in KCl:KH and KCl:KD. Experiments

Yasuhiro Kondo,* J. R. Duffey,† and Fritz Lüty
Physics Department, University of Utah, Salt Lake City, Utah 84112
(Received 22 July 1980)

The doping of KCl with substitutional H^- and D^- ions has been extended from the usual low-concentration "*U*-center" range (10^{-5} to 10^{-3} mole ratio) into the 10^{-2} to 10^{-1} range. This high H^- concentration has made possible Raman measurements of two effects, which so far were not accessible: (1) The H^- defect-induced one-phonon spectrum (0–150 cm^{-1}) which in various scattering geometries displays the coupling of the H^- ion to perturbed phonons of A_{1g}, E_g, and T_{2g} symmetries. (2) A new combination process of the H^- or D^- local mode with lattice phonons, appearing in the parallel scattering geometry as a broad spectrum around 600 and 430 cm^{-1} for H^- and D^-, respectively. Besides these new effects, the second harmonic of the H^- local mode near 1000 cm^{-1} (D^- near 700 cm^{-1}) is observed, split into three components of A_{1g}, E_g, and T_{2g} symmetry, similar to those measured previously for KI:KH and KBr:KH. All three Raman responses scale with the H^- doping for low concentrations, but display at high doping levels marked changes due to H^--H^- interaction. A theoretical treatment of these results is planned to be presented in a separate paper.

I. INTRODUCTION

Negative hydrogen (H^-) ions, substituted for halide ions on lattice sites in alkali halides, are one of the oldest and most extensively studied classes of point defects in solids. From early work in Göttingen the processes involved in the thermal production of these defects were clarified[1] and their uv absorption[2] and photochemical conversion[3,4] properties were systematically studied. More recently the substitutional H^- ions (so-called "*U* centers") became the first defect system for which a high-frequency local mode was discovered.[5] Extended measurements with infrared spectroscopy established the properties of H^- and D^- local modes and their phonon sidebands in a large number of alkali-halide[6] and alkali-earth-halide[7] host crystals. More detailed information was obtained by a reduction of the O_h defect symmetry and splitting of the threefold-degenerate local mode using applied stress,[8] chemical impurities neighboring the H^- ion,[9] formation of H^- pairs,[10] and displacement of the H^- ion on interstitial sites close to the vacancy.[11] This rich experimental material (which always included $H \rightarrow D$ isotope substitution) stimulated extensive theoretical activity, making this simple small mass defect a prototype and model case for the testing of various approaches towards the treatment of local modes[12–14] and their coupling to lattice phonons.[15,16]

Very recently, practical interest in crystals with H^- defects has become strong in connection with the application of color center systems as materials for tunable infrared lasers. The possibility to produce stable and nonaggregated *F* center systems by excitation with x ray,[17] uv,[3] or two-photon exciton absorption[18] in crystals with H^- defects plays a major role in this development, particularly for crystals with spatially modulated coloration as used in distributed feedback color center lasers.[19]

So far all investigations of H^- defects in alkali halides have been performed on very *dilute systems,* restricted in the usually applied technique of *subsequent* additive coloration[20] and hydrogenation to H^- concentrations of $N < 5 \times 10^{-4}$ mole ratio. Though the early work with *simultaneous* additive coloration and hydrogenation showed the feasibility of achieving H^- concentrations up to 10^{-2} in very thin surface layers,[1] this technique was never again systematically pursued and developed further for achieving high H^- amounts in the volume of a crystal. The low-concentration range, available for H^- defects, has excluded the application of experimental techniques like NMR and has discouraged investigations with Raman techniques. As the H^- local mode in an unperturbed crystal is not Raman allowed by symmetry, its observation can only be expected in second harmonics. In the only previous Raman work[21] on dilute ($N < 10^{-4}$) H^- defects in KBr and KI, the second harmonic of the local mode and its splitting due to anharmonicity could be measured. A low-energy gap mode at 95 cm^{-1} in KI was barely detectable, while it was impossible to observe in these dilute systems the one-phonon spectra due to the breaking of translational symmetry by the H^- defects.

In this work we report the first results of a more general attempt to extend the restricted H^- concentration range as far as possible into the alkali-halide hydride mixture. As a first step, we applied and developed in this work the technique of simultaneous

coloration and hydrogenation[1] to its full potential in KCl, achieving an extension of the H^- doping (compared to the "two-step process") by about two orders of magnitude into the 10^{-2} range (Sec. II). These crystals allow easy and precise measurement of various Raman effects connected with the H^- and D^- ions. Besides the second-harmonic local-mode spectra, the defect-induced one-phonon spectra in all polarizations and a new combination effect between local mode and lattice phonons are observed for the first time (Sec. III). A theoretical treatment of these Raman results is planned for a subsequent paper.[22]

II. PREPARATION OF CRYSTALS WITH HIGH H^- CONCENTRATION

The usually applied technique for homogeneous introduction of H^- defects into a crystal is a *two-step process,* consisting of an additive coloration in potassium vapor (reaction 1 in Fig. 1), followed by heating of the crystal in hydrogen gas for conversion of the F center into H^- defects (reactions 2 and 3). As the melting point of the crystal limits the highest achievable potassium concentration [K] in the vapor, the obtained F center and H^- defect concentrations are restricted to $N < 10^{-3}$ mole ratio.

In the *simultaneous coloration and hydrogenation process* the reactions (1), (2), and (3) are proceeding simultaneously. The F centers formed by the "quick" reaction (1) throughout the crystal become converted at the crystal surface by the "slow" reaction with hydrogen into H^- defects, and can be replaced by reaction (1). For a given temperature T {determining [K] (T)} and hydrogen pressure P {determining [H_2] (P)}, an equilibrium value of H^- defects will be established at the crystal surface. Under prolonged treatment with these fixed conditions, the steep diffusion profile of H^- ions at the surface should propagate slowly into the colored crystal.

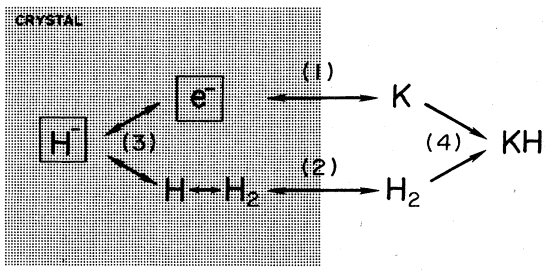

FIG. 1. The four reactions (1 to 4) occurring in the simultaneous coloration and hydrogenation process when a crystal is heated in an atmosphere of potassium vapor (K) and hydrogen gas (H_2).

Two perturbations interfere with a simple extension of these processes to highest pressures and temperatures and long treatment times.

(a) Apparently as the H^- content in the crystal reduces effectively the melting temperature of KCl, *surface melting* can occur. For this reason we had to restrict the crystal temperature to about 50 °C below the melting point of KCl.

(b) Under prolonged heat treatment the potassium and hydrogen *react to form potassium hydride.* After consumption of the potassium by this reaction (reaction 4 in Fig. 1), the vapor pressure of potassium drops and all reactions 1, 2, and 3 will run backwards towards decoloration and dehydrogenation of the crystal.

In the apparatus used for these processes (Fig. 2), the purified potassium metal was placed at the bottom of a nickel container, while the crystals were placed in a covered crucible (with holes) some distance above. After repeated evacuation and purging with dry N_2 and H_2 gas, the container is filled with H_2 gas to 100–300 psi pressure and heated by the oven. The temperature is adjusted to about 725 °C at the level of the crystal, but higher at the bottom level of the container (to maximize the potassium vapor pressure). After a treatment of 10–20 h the crystal can be cooled either quickly or slowly to room temperature. In the case of quick cooling the crystal will contain—besides the achieved H^- defect profile—the high-temperature equilibrium concentration of F centers, too, which are unwanted for our investigation. A slow cooling over several hours in the range 700 → 500 °C, on the other hand, reduces the potassium concentration [K](T) in the vapor and discolors the crystal due to the quick equilibrium reaction (1),

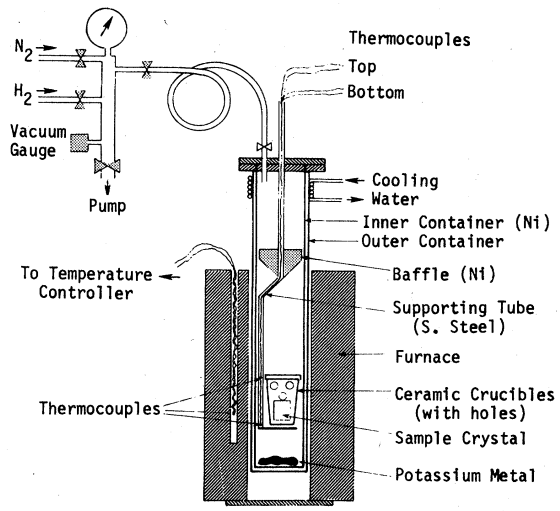

FIG. 2. Schematic illustration of the apparatus used for simultaneous additive coloration and hydrogen treatment.

while affecting the H^- defect profile only in a negligible way.

Three typical profiles of H^- defects as a function of penetration depth, obtained under different conditions of pressure, temperature, and treatment time, are shown in Fig. 3. For the lower concentration sample (1) a uniform hydrogenation over several millimeters can be achieved, while for higher doping an increased variation with depth is observed. For sample 3, treated at the highest temperature and pressure, the hydrogenation profile is extremely steep, producing in a narrow range the highest achieved relative H^- concentration of 8 at.%. Due to the high treatment temperature (740 °C), a partial melting had occurred at the surface, which apparently causes the decrease of the H^- concentration very close to the surface.

The H^- concentration and its spatial profile in the crystal was determined by infrared spectroscopy, using samples of various H^- concentrations (10^{-4} to 10^{-2} mole ratio). The spectrum of the local mode (at $\nu_{LM} = 502\ cm^{-1}$) and its phonon sideband (at $\nu_{SB} = 565\ cm^{-1}$), which is well calibrated for small H^- concentrations,[6] was connected successively to the absorption of more highly doped samples by following the high-energy tail of this absorption. This procedure created the spectral curve in Fig. 4 which spans more than two orders of magnitude in absorption strength. The right-hand ordinate scale indicates the H^- concentrations at which an optical density of one is obtained for a 1-mm-thick crystal. The validity of this optical calibration technique was tested and confirmed by chemical determination of the hydrogen content in some crystal samples.

It is noteworthy that the high-energy tail of the phonon sideband displays over a large range a nearly perfect linear relationship of its logarithmic absorption strength on the photon energy (Fig. 4). Empirically the absorption tail $K(\nu)$ as a function of wave number ν can be described by

$$K(\nu) = K(\nu_{SB}) \exp[-A(\nu - \nu_{SB})] , \quad (1)$$

where ν_{SB} is the wave number (565 cm^{-1}) at the phonon-sideband maximum. The constant A determined from the slope in Fig. 3, is $A^{-1} \approx 63\ cm^{-1}$, which is exactly the energy peak of the phonons coupled to the local mode, or in other words $A^{-1} = \nu_{SB} - \nu_{LM}$. Therefore, we obtain

$$K(\nu) = K(\nu_{SB}) \exp\left[-\left(\frac{\nu - \nu_{SB}}{\nu_{SB} - \nu_{LM}}\right)\right] . \quad (2)$$

If we interpret the sideband and its extended high-energy tail as excitation of the local mode plus $n = 1, 2, 3, \ldots$, phonons of mean energy 63 cm^{-1}, the empirical relation (2) implies an exponential decay of the transition probability with the order n, of the form $K(\nu_n) \propto \exp(-n)$.

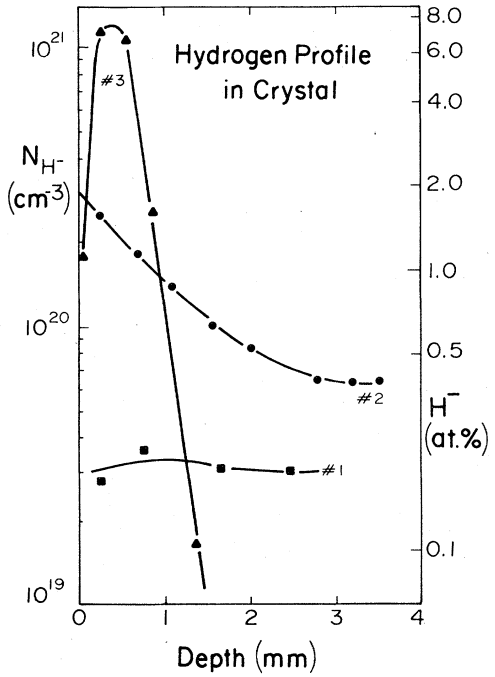

FIG. 3. Profiles of the H^- concentration as a function of the distance from the crystal surface, obtained by infrared measurements in three samples after different types of hydrogenation treatments.

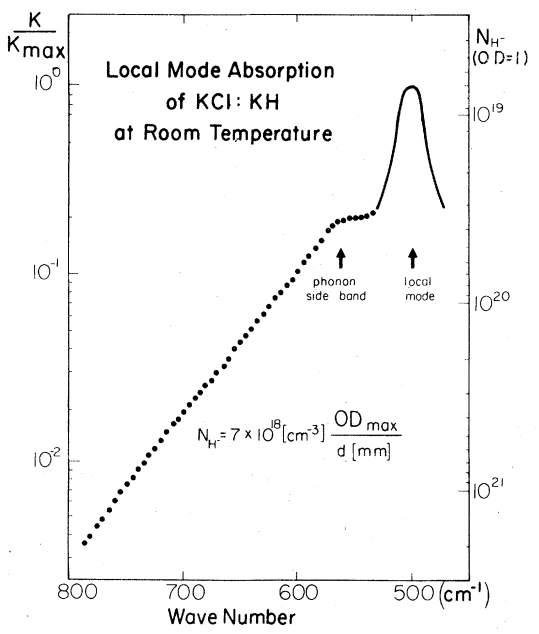

FIG. 4. Room-temperature local mode absorption of KCl:KH (obtained from crystals with various doping). The scale on the right side indicates the H^- concentrations, for which the OD = 1 in a 1-mm-thick crystal.

III. EXPERIMENTAL RESULTS AND THEIR INTERPRETATION

Figure 5 shows a survey of the Raman response of KCl crystals with three different KH concentrations, covering the total investigated spectral range 0–1100 cm^{-1}. The spectra were taken with the scattered light unanalyzed so that all Raman active modes, regardless of symmetry, appear. Five different spectral effects can be distinguished in this survey.

(a) The *second-order spectrum of pure KCl,* indicated by the dotted line, appears in all crystals as the expected host-lattice background. Its prominent peak at ~ 300 cm^{-1} can be used as a reference to which the strength of the defect-induced scattering effects can be compared.

(b) A low-energy spectrum (0–200 cm^{-1}) the strength of which scales linearly with the amount of KH in the crystal. It must be attributed to a *one-phonon spectrum* caused by the presence of the KH. The introduction of the H^- ions into the crystal destroys the lattice periodicity and inversion symmetry of the ions around the defect, thus allowing first-order Raman scattering from phonons throughout the Brillouin zone.

(c) A sharp three-line structure observed at ~ 1000 cm^{-1}. As the infrared active but Raman inactive local mode of H^- in KCl is located near 500 cm^{-1}, the Raman response at 1000 cm^{-1} must be due to the *second harmonic of the H^- local mode.*

(d) The broad spectrum at 600 cm^{-1} scaling with the H^- doping is a new and unexpected effect. Its large width (150 cm^{-1}) indicates that it originates from a broad phonon spectrum. This feature, together with its position at 600 cm^{-1}, suggests strongly that it is caused *by a combination effect of the H^- local mode with lattice phonons.*

(e) A tiny sharp line appears close to 500 cm^{-1} in samples with high H^- concentrations. It must be due to the *fundamental local mode vibration of an H^- ion in some type of perturbed surrounding* which breaks the inversion symmetry and makes the Raman response of the fundamental allowed.

While the well-understood lattice background effect (a) does not need any further attention, we will focus on each of the four defect-induced phenomena (b)–(d) with more detailed measurements and discussions.

Figure 6 shows an unpolarized measurement, similar to the ones in Fig. 5, but performed on a crystal doped with about *equal amounts of KH and KD.* While the one-phonon spectrum is essentially unaffected by the isotope exchange as expected, the defect-induced Raman effects connected with the local mode display a shift to lower energies by a factor close to the inverse square root of the mass ratio $1/\sqrt{2}$. The second harmonic of the D^- local mode appears at 720 cm^{-1} (which corresponds well to the observation of the fundamental local mode at 360 cm^{-1} in the infrared). The broad spectrum at 600 cm^{-1} for KH appears in KD at ~ 430 cm^{-1}. (Both KD spectra are somewhat weaker than the corresponding KH spectra due to the smaller local mode amplitude of the D^- ion compared to the H^- ion.) The $1/\sqrt{2}$ shift of the broad band at 600 cm^{-1} confirms our general assignment of this spectral feature

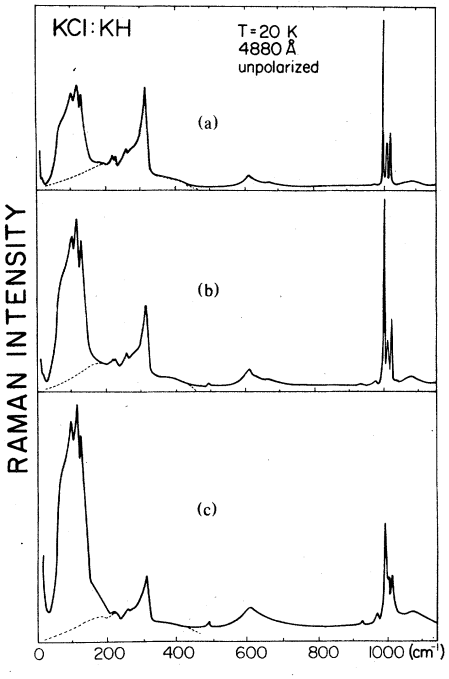

FIG. 5. Unpolarized low-temperature Raman spectra of KCl, doped with three different amounts of KH. (a) 0.5 at.% KH; (b) 1.1 at.% KH; and (c) 1.7 at.% KH.

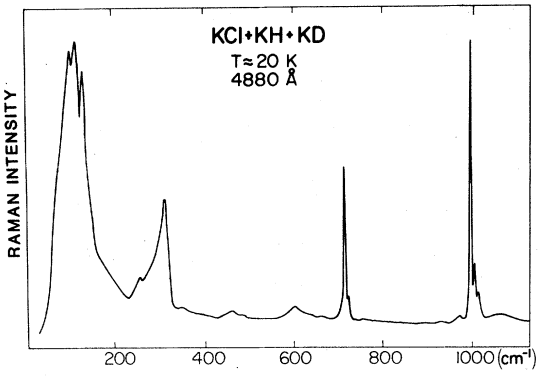

FIG. 6. Unpolarized Raman spectrum of KCl, doped with equal amounts of KH and KD.

to a local mode plus phonons combination effect.

Figure 7 displays the Raman spectra in the *low-energy one-phonon range,* taken for the same crystal in three scattering geometries. The samples for these measurements were cut to present a (110) face which was well polished in order to yield good optical quality. The crystal was oriented in the cryostat so that the laser light is incident along a [001] direction with its polarization being adjustable in [110] and [$\bar{1}$10] crystallographic directions. The scattered light propagates along the [$\bar{1}$10] direction and its polarization is analyzed in [110] and [001] directions. Without moving the crystal, three geometries of incident and scattered polarization ([110][110], [$\bar{1}$10][110], and [110][001]) can be measured, allowing the detection and separation of Raman spectra of all three symmetries. As Fig. 7 shows, one-phonon peaks of A_{1g} symmetry are observed at 100, 113, and 129 cm^{-1}, while for E_g symmetry peaks at 71 and 121 cm^{-1} appear. The Raman contributions of T_{2g} symmetry are rather small and unstructured. The second-order Raman effect from the lattice background with a peak at 315 cm^{-1} appears mainly in the A_{1g} symmetry. The defect-induced one-phonon spectra reflect directly the coupling of the H^- or D^- ion to perturbed phonons of A_{1g}, E_g, and T_{2g} symmetry. The general appearance of these spectra has some similarities to the ones observed for the F center, which has $1s$ and $2p$ electronic states centered at an anion site similar to the H^- defect. In detail, however, differences appear and are expected due to the much more compact wave function of the H^- defect compared to the rather diffuse and extended F-center wave function

Figure 8 displays polarized Raman spectra in the *second-harmonic region of the local mode* taken with an instrumental resolution of 2 cm^{-1}. Experiments with two crystals [having (100) and (110) optical faces] and various scattering geometries lead to consistent results: There is a mode of A_{1g} symmetry at 1005 cm^{-1}, a mode of E_g symmetry at 1014 cm^{-1} and a mode of T_{2g} symmetry at 995 cm^{-1}. As the H^- ion is at a site of cubic (O_h) symmetry, the ground state ($n=0$) wave function will transform as the A_{1g} irreducible representation of the O_h point group, and the $n=1$ excited state as the T_{1u}. The $n=2$ excited state will be split by anharmonic perturbation and transform as the A_{1g}, E_g, and T_{2g} irreducible representation. Owing to the inversion-symmetry transitions between states of different parity will be observed in infrared absorption but not in Raman, while transitions between states of the same parity will be Raman active but infrared inactive. This leads to the single line infrared $n=0 \rightarrow n=1$ transition at

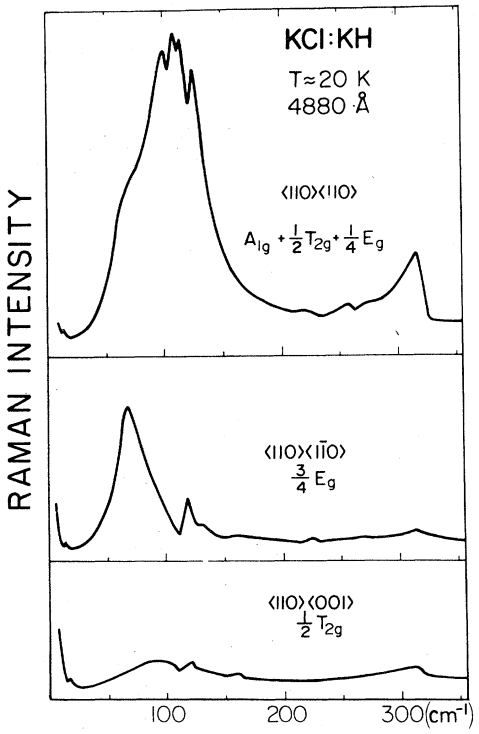

FIG. 7. Raman spectrum of KCl:KH in the low-energy range, taken in three different scattering geometries.

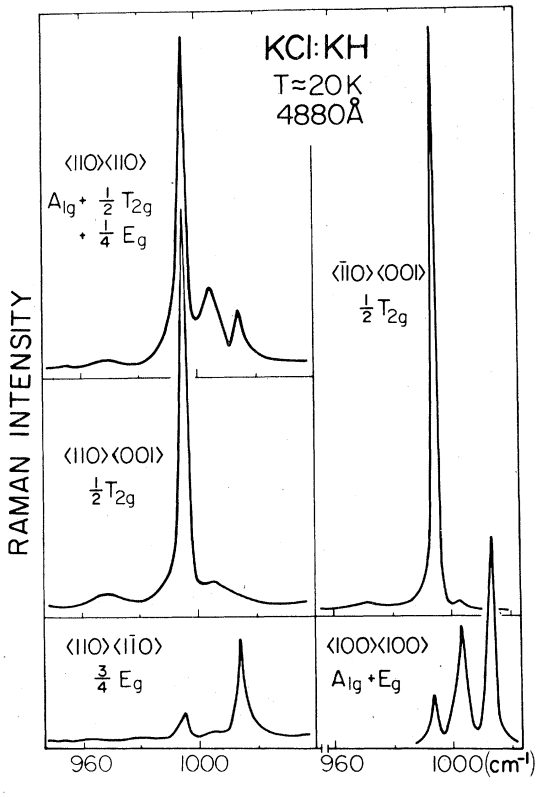

FIG. 8. Raman spectra of KCl:KH in the 1000-cm^{-1} range, taken in five different scattering geometries.

500 cm^{-1}, and the $n=0 \rightarrow n=2$ Raman active transition which splits into components of A_{1g}, E_g, and T_{2g} symmetry.

Very similar Raman results on the second-harmonic H^- local mode have been obtained by Montgomery *et al.*[21] for the system KI:KH and KBr:KH. The spectral sequence with rising energy (T_{2g}, A_{1g}, and E_g) and the splitting between neighboring peaks ($\sim 8-10$ cm^{-1}) is basically the same in both systems, indicating a similar contribution due to anharmonicity. The observed relative intensity of the three bands (T_{2g} about twice as intense compared to A_{1g} or E_g, which have approximately equal intensity) is again similar to the KI:KH and KBr:KH system. This latter point is in contradiction to the calculations,[21] which predict a much stronger scattering from the A_{1g} and E_g modes compared to the T_{2g} modes.

In addition to the material presented in the figures of this paper we have also measured the splitting of the second harmonic of the D^- local mode in KCl. The three components (shown only in poor resolution in the survey measurement Fig. 6) were found to lie at 714, 717, and 724 cm^{-1} for the T_{2g}, A_{1g}, and E_g peak, respectively. According to the theoretical model in Ref. 21, the splitting should vary under $H \rightarrow D$ mass exchange by a factor of 2; i.e., $\Delta\nu(H^-):\Delta\nu(D^-)=2$. For the H^- mode in KCl we found $\Delta\nu(E_g - T_{2g})=19$ cm^{-1} and $\Delta\nu(A_{1g}-T_{2g})=10$ cm^{-1}. The corresponding $\Delta\nu$ values for the second harmonic D^- local mode are 10 and 3 cm^{-1}, respectively, in fairly good agreement with the predicted reduction by a factor of 2 due to the mass substitution. [The somewhat too small value $\Delta\nu_{D^-}(A_{1g}-T_{2g})=3$ cm^{-1} might be caused by interaction effects in the highly doped samples used, as will be discussed later in conjunction with Fig. 11.]

Figure 9 displays polarized Raman spectra of KCl:KH in the spectral region of the *combination effect at 600 cm^{-1}*. The $A_{1g}+E_g$ spectrum was taken with a cleaved ⟨100⟩ crystal (for better optical quality and signal-to-noise ratio), while the T_{2g} and E_g spectra were obtained with ⟨110⟩-cut crystals as described above. As Fig. 9 shows, the combination effect is predominantly of A_{1g} symmetry, showing a strong main peak at 607 cm^{-1} and a side peak at 660 cm^{-1}. While there appears to be no contribution of T_{2g} symmetry, a weak E_g response (in the same range as the A_{1g} spectrum) is barely detectable.

As mentioned earlier in the survey of all the Raman effects (Fig. 5), a very weak *sharp line structure* was observed in the crystals with highest KH doping *in the 500-cm^{-1} region*. Figure 10 shows this effect in an expanded scale. Two sharp lines are visible, one at 488 cm^{-1} (of A_{1g} or E_g symmetry), and one at 483 cm^{-1} of T_{2g} symmetry. It is evident that this weak line spectrum must originate from the fundamental local mode of an H^- ion located at a perturbed site of

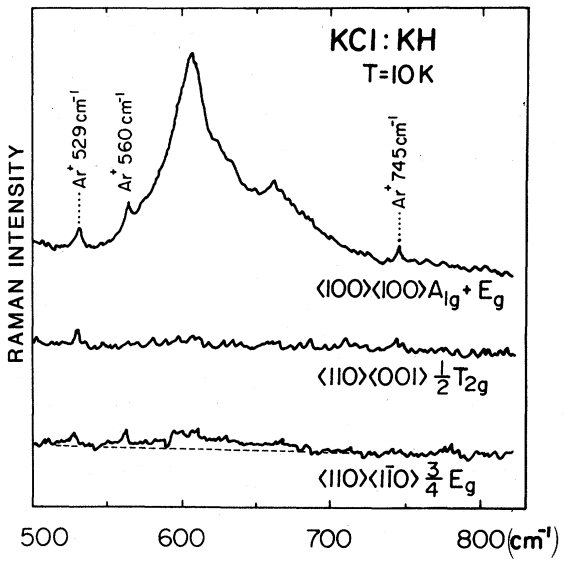

FIG. 9. Raman spectra in the range of the 600-cm^{-1} combination effect, measured in three scattering geometries. (The three weak Ar^+ plasma lines supply accurate wavenumber calibration.)

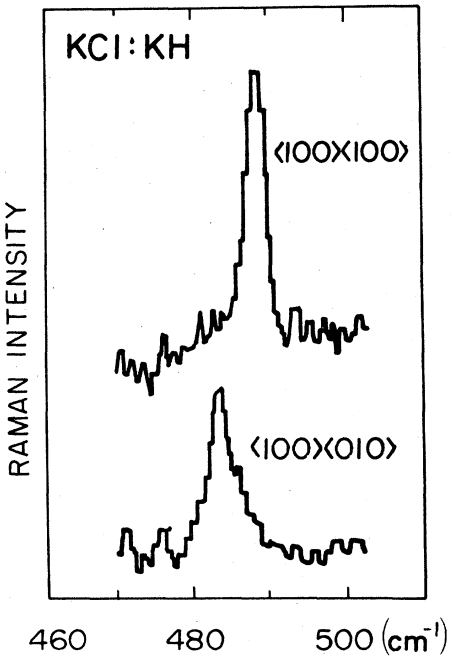

FIG. 10. Raman spectrum in the range of the H^- fundamental local mode frequency (~ 500 cm^{-1}), measured at 10 K for two polarization geometries in KCl with high KH doping.

broken inversion symmetry. A point defect, neighboring the H^- ion, would achieve this. As the host crystals contain an estimated chemical impurity level of $N_{imp} < 100$ ppm it is evident that the H^- ions themselves are by far the predominant candidates qualifying to be neighboring impurities of the H^- defect. For a doping level of 3 at.% and random H^- distribution, the probability for having one of the twelve next-nearest-neighbor places of an H^- ion occupied by another H^- ion is $(0.03)(12) = 0.36$, so that over one-third of the defects should be present in the form of pairs. $\langle 110 \rangle$-oriented pairs of H^- defects have been identified and studied previously by polarized infrared spectroscopy.[10] The observed splitting of the degenerate H^- local mode into three components could be fitted and accounted for by a simple oscillator model with slightly changed effective force constants due to electric dipole coupling between the two H^- oscillators.

Aside from the three infrared-active in-phase modes of the pair, three out-of-phase pair modes exist, which should be Raman active. The model in Ref. 10 predicts these modes for KCl:KH to lie at about 538, 467, and 491 cm^{-1}. The 538-cm^{-1} mode, due to the longitudinal stretching vibration of the pair, would be expected to appear in parallel-polarized Raman scattering, while the two transversal 467 and 491^{-1} modes should appear in perpendicular scattering. In spite of the high concentration of pairs in our crystals, none of these modes was observed. From the infrared work, the existence of the pairs and their modes (with sizable frequency shifts) is well established. Therefore the only explanation for not observing them must lie in an extremely small first-order Raman efficiency. Unlike the atoms in an H_2 molecule, the two H^- ions on neighboring $\langle 110 \rangle$ places have a large separation ($d = 4.4$ Å) and little overlap of their individual wave functions. Moreover, the closed-shell electronic structure and ion size of the H^- and Cl^- ions are similar. Therefore the changes in electronic polarizability when an H^- ion moves towards an H^- or a Cl^- ion can be nearly identical so that no observable first-order Raman effect occurs.

This latter argument is consistent with the observations on the *electronic absorption properties* of the crystals with high KH doping. If any sizable overlap or interaction between the electronic wave functions of neighboring H^- ions would be present, a changed electronic absorption should be present for the pair compared to the individual ions; specifically one would expect a lower-energy transition polarized parallel to the pair axis (as in the low-lying M-band transition of the $\langle 110 \rangle$ F-center pair equal to an F_2 center). The uv absorption of the heavily H^--doped crystals, however, showed essentially only the tail of a large U-band absorption, as expected for individual H^- defects. Therefore the electronic absorption (and polarizability) properties of H^- ions in pairs (or larger clusters) are evidently close to those of isolated H^- defects, which agrees with the negative Raman result on the pair modes.

This leaves the question of the origin of the weak Raman line in Fig. 10 open: What other impurity could break the inversion symmetry more effectively than a neighboring H^- and thus produce a small first-order local-mode Raman response? To answer this question, we doped crystals before the hydrogenation with various cationic and anionic impurities (Na^+, Br^-, I^-, OH^-), which in small amounts could be present in the pure crystals. None of these impurities produces any new Raman response close to the local-mode frequency. In a series of further experiments, we applied high electric fields (up to $\sim 10^5$ V/cm) to the crystal, checking carefully the Raman response in the 500-cm^{-1} range for a possible increase of a signal due to the field-induced broken inversion symmetry. The result was negative. Neither the electric field nor the perturbation by a neighboring impurity is sufficient to produce a first-order Raman responose of the H^- local mode.

It should be mentioned in this connection that experiments in the infrared, which are related, have also been negative.[9] In the infrared, the first harmonic of the local mode is allowed and strong, and the second harmonic is not allowed and not observed. Lowering of the H^--doped symmetry (e.g., by a neighboring Na^+ or Rb^+ defect in KCl) leads to a sizable splitting of the local mode absorption (by about 10–50 cm^{-1}). In spite of the fact that about 30% of the H^- defects had been attached to Na^+ impurities, no second-harmonic absorption of the local mode could be detected.[9] In agreement with this, our highest H^--doped (~ 3 at.%) samples (in which about one-third of the hydrogen should be in the form of pairs) did not show any trace of a second harmonic local mode infrared absorption. This demonstrates that even if neighboring impurities split and shift the local mode frequency by sizable amounts, the oscillatory motion of the H^- remains harmonic. Consequently, the vibrational amplitude of the H^- when approaching the impurity and when moving away from it must be exactly the same. This helps to understand that the change in electronic polarizability during the two half-cycles of the vibration are exactly equal too, so that no first-order Raman response is observed.

The only way in which an H^- local mode *has* been observed in first-order Raman was by resonance Raman excitation of an F center located in a $\langle 110 \rangle$ neighboring position beside an H^- defect ("F_H center").[23] The diffuse $1s$ and $2p$ wave functions of the F center overlap the region of the H^- defect, so that due to the strong electron-phonon coupling the H^- local mode appears in the Raman spectrum of the perturbed F center. We believe that the weak Raman

lines in Fig. 10 originate in a similar way from very small amounts of color centers coupled to the H^- local modes which are excited in resonance by the laser light. This interpretation is supported by the observation that in crystals of extremely high H^- concentration, intense blue laser light is sufficient to produce a weak coloration of the crystals. This could be observed by the appearance of a weak orange-red luminescence, indicating the presence of small amounts of F_2^+ centers in the crystal. It is therefore likely that the Raman structure in Fig. 10 is not due to excitation of the H^- electron, but due to resonance-enhanced excitation of some neighboring color center electron coupled to an H^- defect.

The larger-scale goal under which we set out has not yet been reached: To leave the concentration range of H^- defects and to progress through the regime of truly mixed alkali-halide hydrides as far as possible towards the pure alkali hydrides. If this would be possible, the gradual evolution from the localized vibrations of individual H^- defects into the high-frequency collective modes of the H^- sublattice could be studied: first through a mixed spatially disordered phase, and converging into the pure alkali-hydride behavior. We are actively working to progress in this direction.

In the presented work we have not yet left the concentration regime in which the H^- response can be treated basically by that of individual uncoupled defects. Even for the highest achieved H^- concentrations, the low-energy one-phonon spectrum and the combination effect of 600 cm^{-1} show only a minor washing out of fine structure. The second harmonic local mode response shows the most definite changes with concentration (Fig. 11): All three components broaden and shift to higher energies, showing the effects of interaction among the H^- ions. The basic description of the response as a local mode, split by anharmonicity into three components of A_1, E_g, and E_{2g} symmetry remains valid, however.

The achieved increase of H^- concentration has brought about two important features, which were not observable before: The Raman spectra of the perturbed lattice phonons coupling to the H^- defect, and the new Raman combination effect between H^- local mode and ungerade lattice phonons. Both these effects will be treated theoretically in a planned seperate paper.

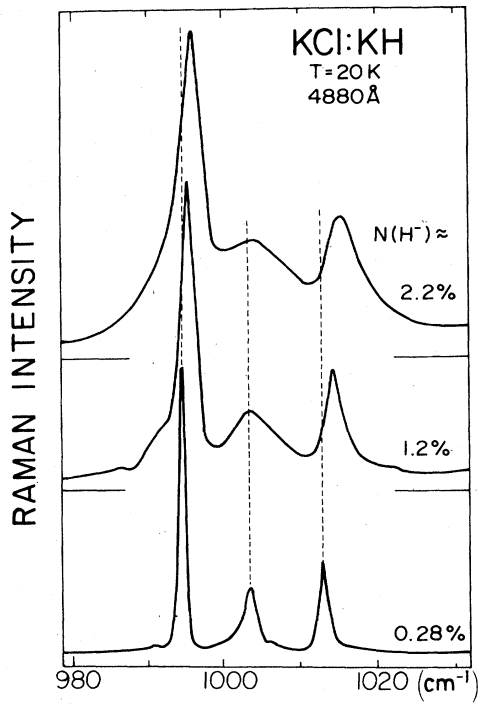

FIG. 11. Unpolarized Raman spectra of KCl:KH in the 1000-cm^{-1} range, taken for three different amounts of KH doping.

ACKNOWLEDGMENT

Work supported by the NSF Grant No. DMR 77-12675.

*Present address: Institute for Solid State Physics, University of Tokyo, Tokyo 106.
†Present address: Hughes Aircraft Company, Culver City, Cal. 90230.

[1]R. Hilsch, Ann. Phys. (Leipzig) 29, 407 (1937).
[2]R. W. Pohl, Phys. Z. 39, 36 (1938).
[3]R. Hilsch and R. W. Pohl, Ann. Phys. (Leipzig) 32, 156 (1938).
[4]C. J. Delbecq, B. Smaller, and P. H. Yuster, Phys. Rev. 104, 599 (1956).
[5]G. Schaefer, J. Phys. Chem. Solids 2, 233 (1960).
[6]For a review of this work see B. Fritz, in *Localized Excitations in Solids*, edited by R. F. Wallis (Plenum, New York, 1968).
[7]W. Hayes, M. C. K. Wiltshire, D. Jumeau, and L. Taurel, Phys. Status Solidi B 67, 239 (1975).
[8]B. Fritz, J. Gerlach, and U. Gross, in *Localized Excitation in Solids*, edited by R. F. Wallis (Plenum, New York, 1968).
[9]W. Barth and B. Fritz, Phys. Status Solidi 19, 515 (1967).
[10]M. de Souza and F. Lüty, Phys. Rev. B 8, 5866 (1973).
[11]B. Fritz, J. Phys. Chem. Solids 23, 375 (1962).
[12]T. Timusk and M. V. Klein, Phys. Rev. 141, 664 (1966).
[13]R. Wallis and A. A. Maradudin, Prog. Theor. Phys. 24, 1055 (1960).

[14]J. B. Page and D. Strauch, Phys. Status Solidi 24, 469 (1967).
[15]T. Timusk and M. V. Klein, Phys. Rev. 141, 664 (1966).
[16]J. B. Page and B. G. Dick, Phys. Rev. 163, 910 (1967).
[17]W. Martienssen, Z. Phys. 131, 488 (1952).
[18]L. F. Mollenauer and W. J. Tomlinson, Phys. Rev. Lett. 35, 1662 (1975).
[19]G. C. Bjorklund, L. F. Mollenauer, and W. J. Tomlinson, Appl. Phys. Lett. 29, 116 (1976).
[20]H. Rögener, Ann. Phys. (Leipzig) 29, 386 (1937).
[21]G. P. Montgomery, W. R. Fenner, and M. V. Klein, Phys. Rev. B 5, 3343 (1972).
[22]M. Portney and J. B. Page, Bull. Am. Phys. Soc. 24, 442 (1979); and (unpublished).
[23]D. Pan and F. Lüty, Phys. Rev. B 18, 1868 (1978).